ART. N° 451
Contribution COB N° 627

From: MARINE GEOLOGY AND OCEANOGRAPHY OF THE PACIFIC MANGANESE NODULE PROVINCE
Edited by James L. Bischoff and David Z. Piper
(Plenum Publishing Corporation, 1979)

INFLUENCE OF DEEP WATER CIRCULATION AND SEA FLOOR MORPHOLOGY ON THE ABUNDANCE AND GRADE OF CENTRAL SOUTH PACIFIC MANGANESE NODULES

Guy Pautot and Marthe Melguen

CNEXO - Centre Océanologique de Bretagne
B.P. 337 - 20273 Brest Cedex, France

Abstract

— Analyses of polymetallic nodules from the central south Pacific and from the underlying sediments indicate that nodule abundance is at least partly related to the degree of carbonate dissolution, which, itself, is strongly influenced by the flow of the Antarctic Bottom Water. The greatest nodule abundance is generally encountered in a 300 to 400 meter thick water layer situated between the lysocline and the calcite compensation depth levels. This range of depth is the first and main controlling factor of abundance. Inside this range, the bathymetry represents a secondary factor influencing both abundance and grade. Some correlations appear locally between nodule grade and abundance. Nodule grade seems to be generally related to the bottom morphology. Ni, Cu and Mn grades are positively correlated and are highest in topographic lows. On the contrary, Co and Cu are negatively correlated and Co presents higher grade on topographic highs. —

Introduction

Recent studies undertaken by the Centre National pour l'Exploitation des Océans (Pautot and Hoffert, 1974; Pautot and Melguen, 1975; Pautot and Melguen, 1976) have stressed the importance of the environment of polymetallic nodules in the Central South Pacific.

Contribution n° 627 du Département Scientifique du Centre Océanologique de Bretagne.

Structural Framework of the Studied Area

The Tuamotu Archipelago (Fig. 1) bound in the North by the Marquesas fracture zone, has been mapped in a general way by Menard (1964), Mammerickx et al. (1975) and in more detail by Monti and Pautot (1974). The Marquesas fracture zone (Fig. 1) was described by Menard (1964) and mapped by Mammerickx et al. (1972). The Marquesas Islands Archipelago (Fig. 1), composed of a modern (Plio-Pleistocene) volcanic mass (Duncan and McDougall, 1974), is about 500 km long and is oriented NW-SE. The Society Islands Archipelago is part of a complex similar in size to the Marquesas Archipelago and with a trend which is nearly parallel.

The Tiki and the Tapu Basins (Figs. 2, 3) respectively situated to the south and west of the Marquesas Islands, correspond to two large depressions (water depth respectively greater than 4000 m and 5000 m) with respect to the average water depth in the studied area.

The Austral-Cook Archipelago (Fig. 4) extending from the Cook Islands to the Tubuai Islands, is oriented in the same direction as the Tuamotu Archipelago and is cut by Austral-Mururoa Fracture zone.

CENTRAL SOUTH PACIFIC

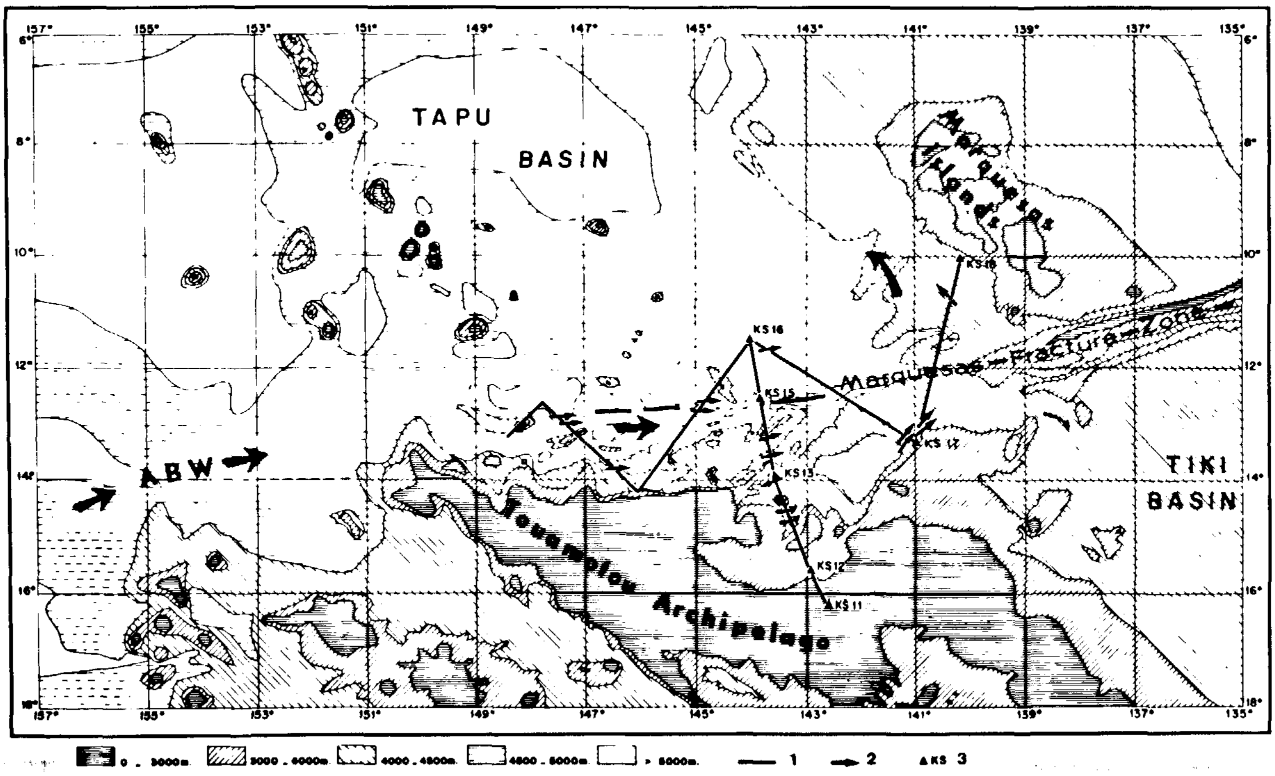

Fig. 1. Schematic map from the Tuamotu-Marquesas area after bathymetric maps from Monti and Pautot (1974). Areas with different depths levels are represented by different symbols. 1: tracks from O.V. Le Noroit during Transpac I cruise. 2: erosion features determined on seismic profiles. KS: position of gravity cores. Big arrows and dotted arrows represent hypothetical flow of AABW (Antarctic Bottom Water).

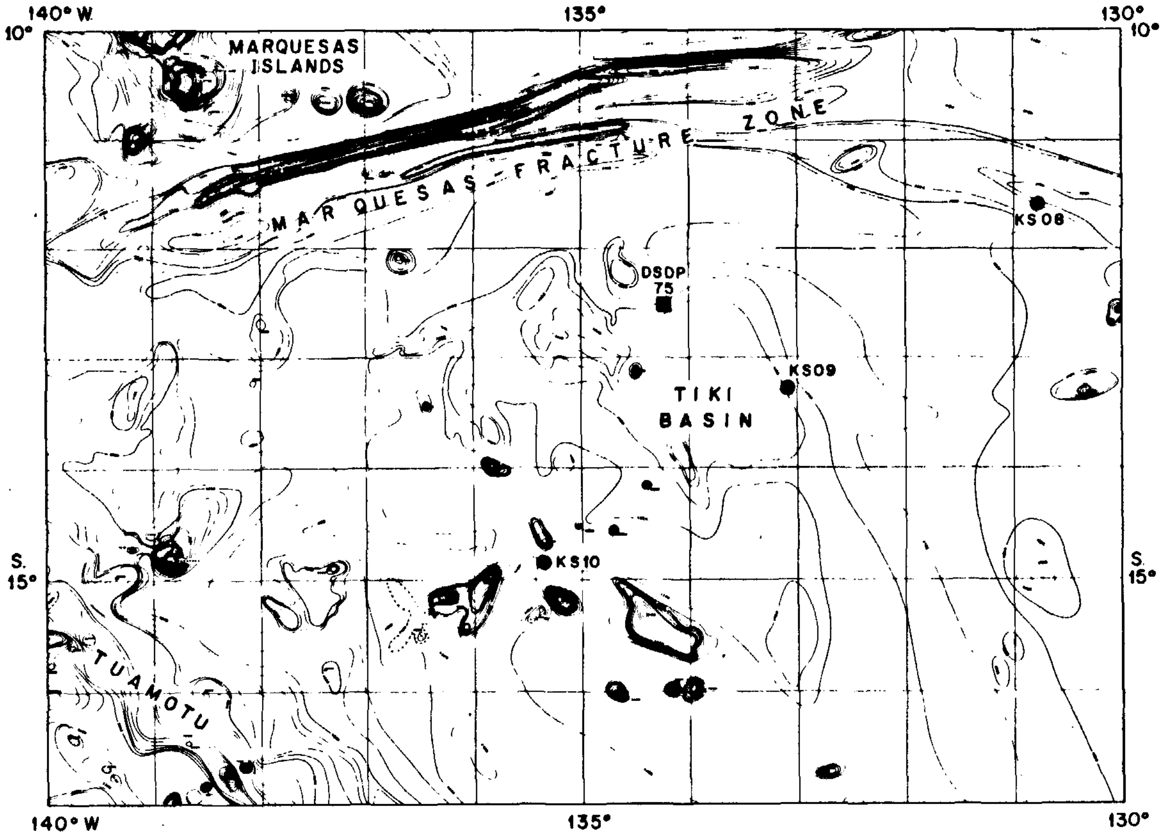

Fig. 2. Bathymetry of the Tiki Basin (after Monti and Pautot, 1974) with positions of cores (KS) taken during TRANSPAC I cruise.

The Aitutaki Area (Fig. 4, 5), situated between the western end of the Southern Cook Islands and the Manihiki Plateau, has been mapped by Mammerickx et al. (1975). A deep channel in this area was named Aitutaki Passage by Pautot and Melguen (1976) after the name of the nearest island.

The Tonga Area (Fig. 5), is located east of the Tonga trench and south of 20° S. Water depth is in general greater than 4500 m.

Objectives

The purpose of this study is to examine our previous hypothesis (Pautot and Melguen, 1976) that the nodule distribution is closely linked to the distribution of the Antarctic Bottom Water and, therefore, to the hydrographic lysocline level as defined by Peterson (1966) and later discussed by Heath and Culberson (1970), Edmond (1971) and Berger (1974).

New data concerning the environment, distribution and composition of the nodules in the Central South Pacific have now been kindly made available to us by the CNEXO/SLN group[1] and AFERNOD[2].

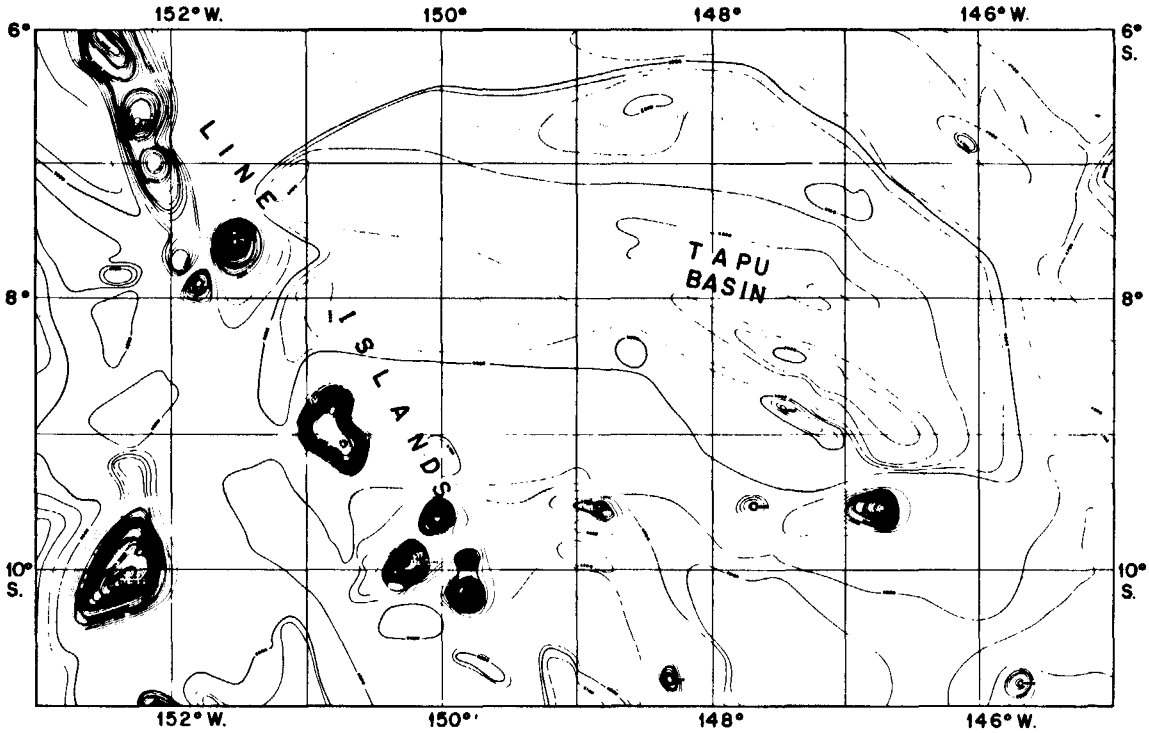

Fig. 3. Bathymetry of the Tapu Basin (after Monti and Pautot, 1974).

We also received samples (nodules and sediments) from the ORSTOM[3] Noumea team. The new data, associated with older results obtained during CNEXO/COB[4] cruises TRANSPAC I (Panama-Tahiti) and TRANSPAC II (Mururoa-Callao), have allowed us to further test our previous hypothesis and to study the importance of bottom topography on nodule abundance and grade.

Present South Pacific Patterns

Antarctic Bottom Water Circulation

The course of the Antarctic Bottom Water in the South Pacific has been described, at least partially, by Wooster and Volkman (1960) and more recently by Reid et al. (1968), Edmond et al. (1971), Johnson (1972), Hollister et al. (1974).

---

[1] Group: Centre National pour l'Exploitation des Océans/Société Le Nickel.
[2] Association Francaise pour l'Etude et la recherche des Nodules Polymétalliques.
[3] Office de la Recherche Scientifique des Territoires d'Outre-Mer.
[4] Centre Océanologique de Bretagne.

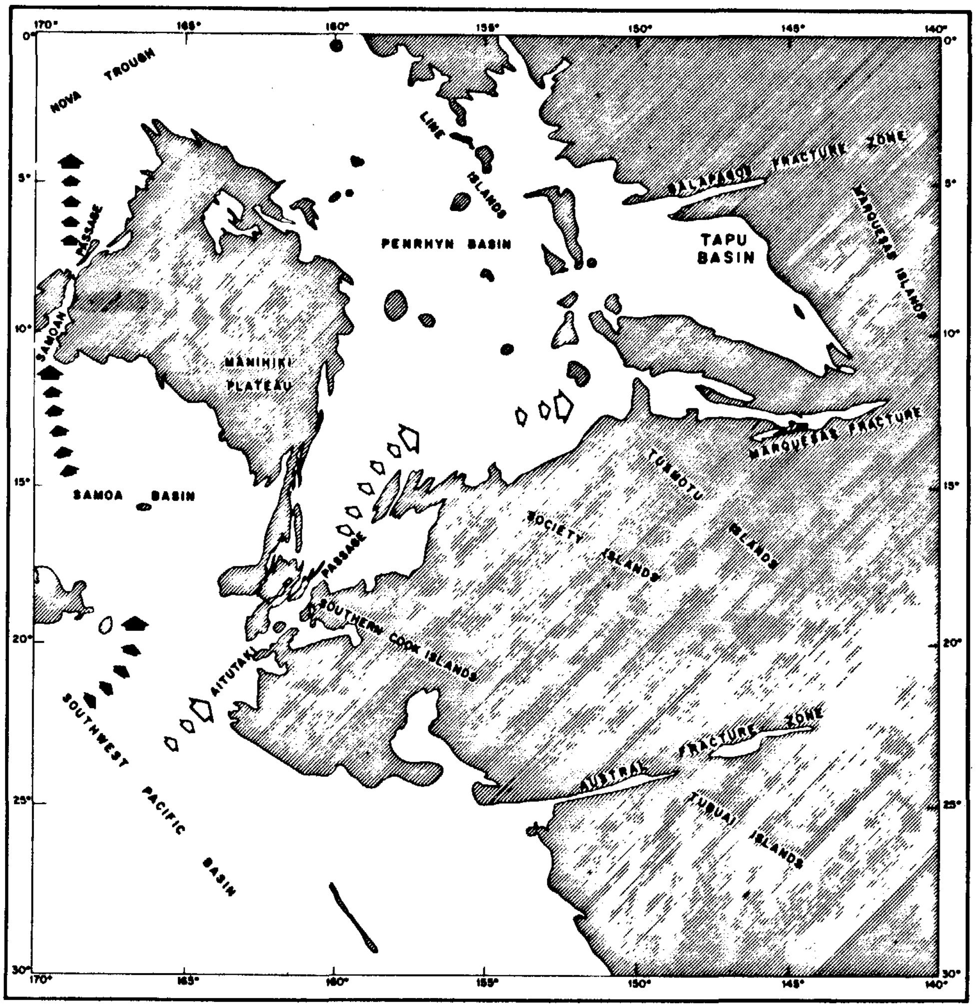

Fig. 4. General map of the whole studied area. Dashed areas are shallower than 2600 fathoms. Dark arrows are representing well-known flow of AABW. White arrows are representing the hypothetical secondary flow of AABW to the East.

The Antarctic Bottom Water AABW enters the Pacific south of Tasmania and crosses the Pacific Rise by way of fracture zones and basins at depths greater than 4000 m. From the Tonga-Kermadec trench, it flows into the Samoan Basin (Fig. 4) and then into the North Pacific through the Samoan Passage (Reid and Lonsdale, 1974). However, all the AABW reaching the Samoan Basin does not flow through the Samoan Passage. The Aitutaki Passage is a second passage (Pautot and Melguen, 1976) that may permit a branch of the Antarctic Bottom Current to reach the Penrhyn Basin and also the Marquesas fracture zone and extend into the Tiki and Tapu Basins (Fig. 4). Abundant erosional structures have been revealed by bathymetric and geophysic observations along different profiles (Fig. 6) crossing the Marquesas fracture zone area. Erosional channels, in sedimentary strata, cut by near-bottom currents, are common all along the fracture zone (Pautot and Melguen, 1976), but only in water depths greater than 4000 m.

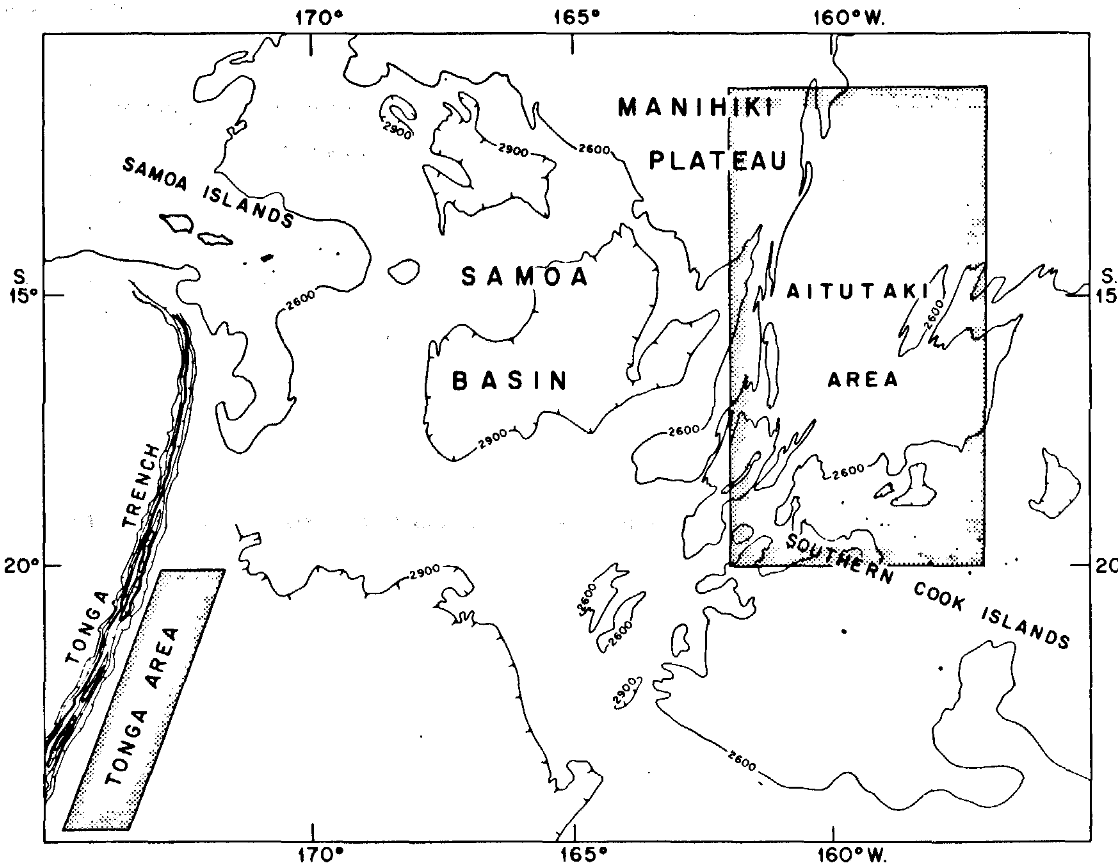

Fig. 5. Map of the Cook-Manihiki area (after Mammerickx et al., 1975). Aitutaki and Tonga areas are two of the areas studied in this paper.

No current measurements are available in the Aitutaki Passage, but a bottom water potential temperature measurement (1.08° C; Wooster and Volkman, 1960) is close to the temperature (0.8° C) (Craig et al., 1972) of the Antarctic Bottom Water flowing through the South West Pacific Basin. According to Craig et al. (1972), the temperature of the AABW varies between 0.6° C in its deepest part to approximately 1° C at its upper limit (Fig. 7). The upper limit is not always well defined because of the presence of a transition layer (600 m thick) separating the AABW, also called Pacific Bottom Water (PBW), from the shallower Pacific Deep Water (PDW). The upper surface (3380 m) of the transition layer, which is defined by the upper inflection point (Fig. 7) is called the "benthic front" and may correspond to the "depth of no motion" between the water masses.

The AABW is one degree colder, much more oxygenated, and consequently much more aggressive with respect to calcium carbonate than the PDW. Near-bottom potential temperature of 0.83° C measured at 5500 m water depth (Reid and Lonsdale, 1974) in the Penrhyn Basin must reflect the flow of PBW in that basin. This is in accordance with the observations of Wong (1972) who suggested the presence of

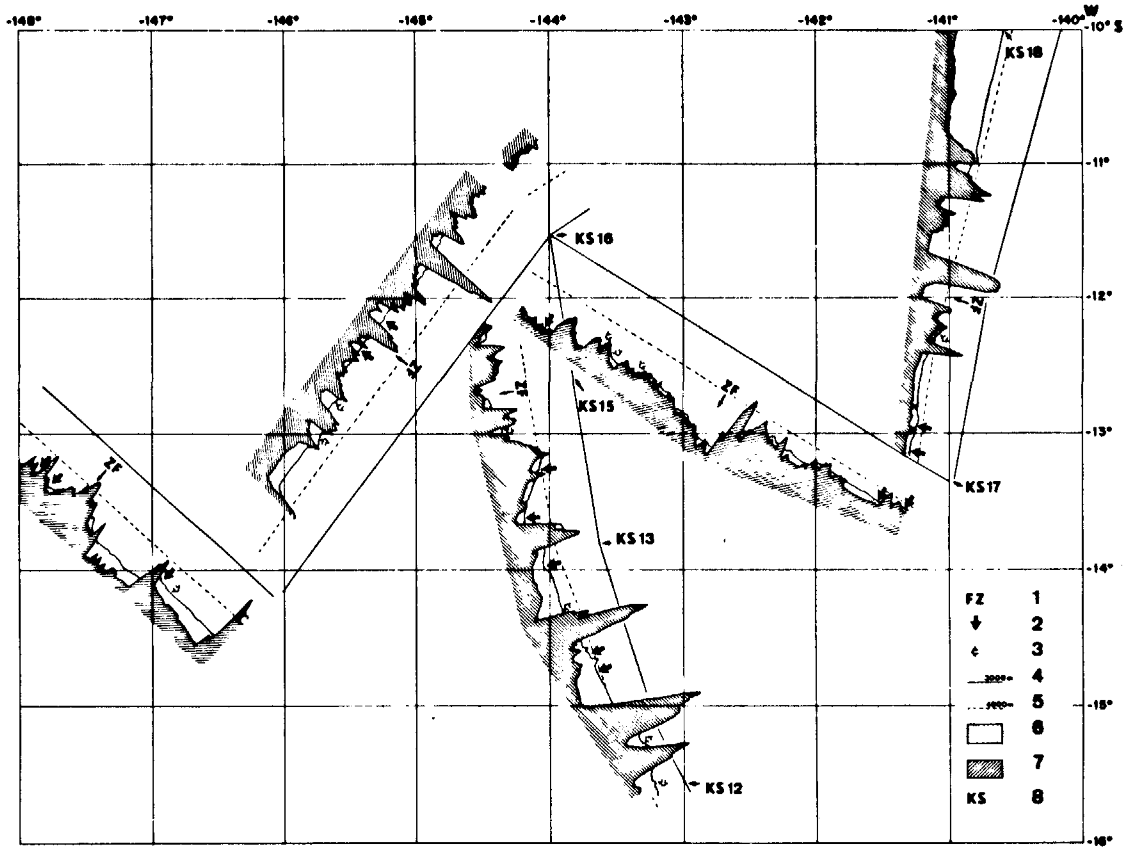

Fig. 6. Seismic profiles carried out during TRANSPAC I cruise along Marquesas Fracture Zone. Position of the tracks are drawn on Fig. 1. 1. Axis of the Fracture zone. 2. Deep erosional sedimentary features. 3. Slump sedimentary features. 4. Position of track line representing 3000 m isobath. 5. 4000 m isobath. 6. Sedimentary cover. 7. Acoustic substratum. 8. Location of gravity cores.

the AABW in the Penrhyn Basin, and between the Galapagos and the Marquesas fracture zones (from 5° to 10° S and up to 130° W). The Tapu Basin (west of the Marquesas Islands and south of the Galapagos Fracture Zone) can be reached by this flow because the Line Islands do not constitute a continuous barrier.

The Marquesas Fracture Zone is represented by a deep channel as far as the southernmost part of the Marquesas Islands. An incursion of the AABW along the Marquesas Fracture Zone and then in the Tiki Basin is thus possible.

Hydrologic measurements were made during the TRANSPAC cruises. In the Marquesas Fracture Zone we did not obtain bottom (5000 m) temperature measurements, but at 3800 m depth the potential temperature was 1.68° C whereas in the neighborhood the bottom temperature is constant around 1.79° C. This value is not a final argument for the presence of the AABW, but according to the observations of Craig et al. (1972), it very probably reflects the presence, at this depth, of the "transition layer" in the Marquesas Fracture Zone.

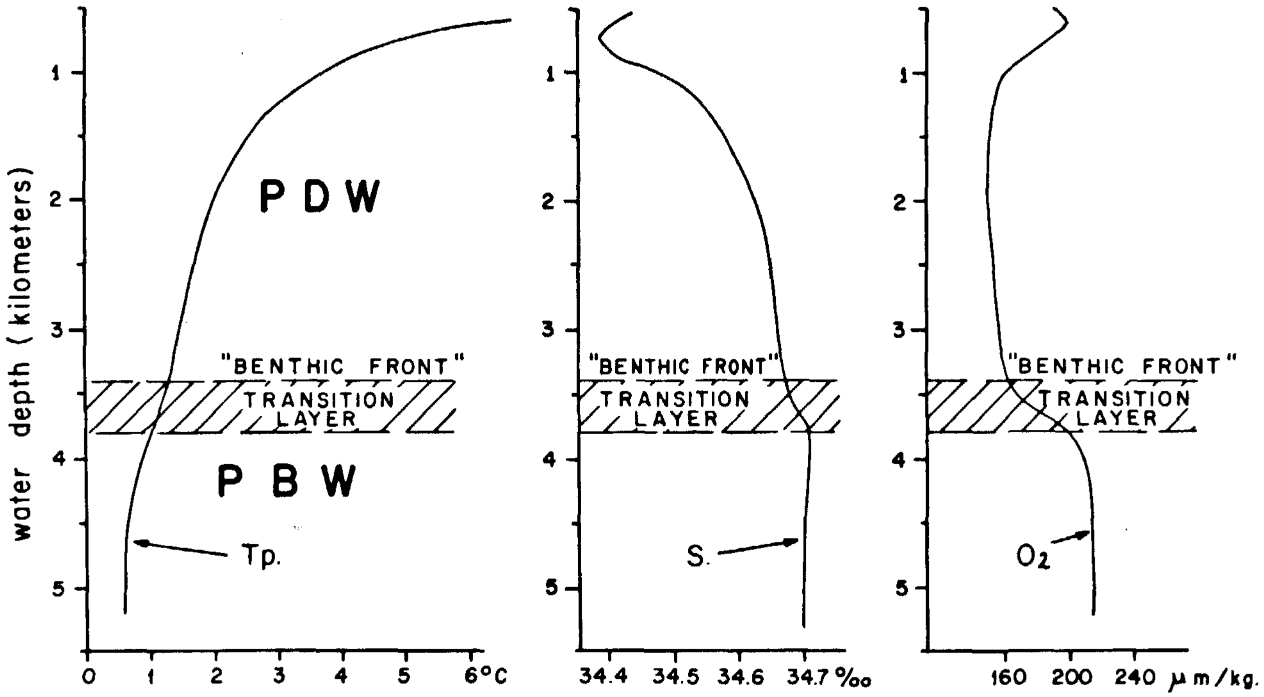

Fig. 7. Depth of the benthic front and of the transition layer separating the Pacific Bottom Water (PBW) from the Pacific Deep Water (PDW). tp: temperature; S: salinity; O_2: oxygen content. After Craig et al. (1972).

Sedimentary Facies Sampling and Analytical Methods

Surface sediments and nodules were collected by means of free-fall grabs. Subsurface sediments were sampled by piston-cores. Sample and core location and depth are given in Appendix Table 1.

A visual examination of the samples and cores was first done using the Munsell color chart. We then studied the sediment composition (including $CaCO_3$ content) and texture by means of smear slides. The Terry and Chilingar (1955) chart was used for estimating the components' frequency. Results of the microscope analysis are given in Appendix Table 2. Sedimentary facies were characterized according to the DSDP classification (Bolli et al., 1978, p. 27-28) which has been slightly modified. Four groups (< 10%, 10-30%, 30-60%, and > 60%) of components' frequencies were considered for siliceous as well as calcareous particles. According to these divisions five lithologic types were considered (see lithologic classification next page).

If nannoplankton is the dominant species in a calcareous ooze, the facies will be called a foram/nanno ooze. The second term is the dominant one. For minor, but very significant components, such as zeolites, hydroxides or volcanic glass, two specific terms were used:

- "bearing", which means containing from 5 to 10%,
- "rich", which means containing from 10 to 20%.

Lithologic classification

% biogenic siliceous particles	Lithologic type
< 10 %	Pelagic clay to siliceous debris-bearing pelagic clay.
10 - 30 %	Siliceous mud.
% biogenic calcareous particles	
< 10 %	Pelagic clay to carbonate debris-bearing pelagic clay.
10 - 30 %	Calcareous mud.
> 60 %	Calcareous ooze.

Age determinations (partly done by C. Müller) were based on calcareous nannoplankton associations, in reference to the associations described by Martini (1971). Much of the sediment was however devoid of calcareous nannofossils. A detailed analysis of the mineralogy, metal content and carbonate content of the surface sediments of the Tiki Basin was done at the Institut de Géologie de Strasbourg (Hoffert et al., internal report, 1978).

Sedimentary Facies Distribution

In the Tuamotu Archipelago-Marquesas Islands area piston-cores were taken along five profiles crossing the Marquesas fracture zone (Figs. 1, 6, 8, Appendix Table 1). Figure 8 gives an example of all the types of sedimentary facies encountered along the N-S profile going from the Tuamotu Archipelago to the North of the Marquesas Fracture Zone. Three major types of sediments were encountered: calcareous turbidites, calcareous mud/nanno ooze and pelagic clay.

Calcareous turbidites are frequent at the base of the Tuamotu Archipelago (cores KS 11 and 12; Appendix Table 2; Fig. 8) as well as at the base of the Marquesas Islands (ex. core KS 18, Appendix Table 2). They are characterized by a high carbonate content (> 60%) abundant and well preserved planktonic foraminifera associated with calcareous algae despite the relatively great (2594-3650 m) water depth. These sediments do not contain metal hydroxides.

The association calcareous mud-nanno ooze is present in core KS 13, as well as in core KS 17 (Appendix Table 2; Figs. 1, 8). The Pleistocene calcareous mud is separated from the Oligocene ooze by a hiatus. Nannoplankton (< 30%) and planktonic foraminifera (< 5%) in surface sediments of these cores, respectively taken at 4350 and 4125 m water depth, indicates that the CCD on the edge of the Tiki Basin is much deeper than 4350 m.

Pelagic clays are the most common facies throughout the studied area (cores KS 15 and KS 16; Appendix Table 2, Fig. 8). They are

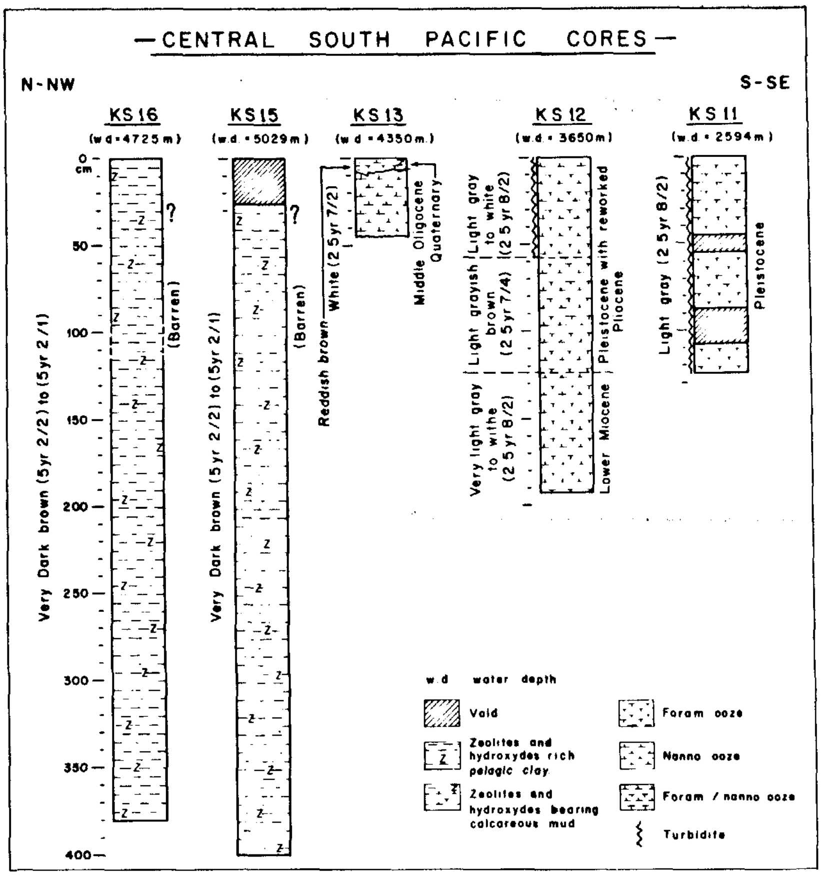

Fig. 8. Facies distribution along five piston-cores taken along a profile (Fig. 1) going from the Tuamotu Archipelago to the N-NW. The different facies types encountered throughout the studied area are present along these cores.

extremely homogeneous and rich in hydroxides (< 20%) and zeolites (< 25%). The lack of $CaCO_3$ in surface sediments of core KS 15 (taken at 5029 m water depth) and the presence of 2% of $CaCO_3$ in core KS 16 (taken at 4725 m water depth) allows us to assume that the CCD here is shallower than 5000 m but very close to 4800 m.

In the Tiki Basin (Figs. 1, 2) surface sediment characteristics (such as $CaCO_3$ content, sand fraction content, Si, Fe, Mn content) have been tentatively mapped by Hoffert et al. (1978, internal report). Calcium carbonate is abundant (> 60%) on topographic highs (water depth > 4200 m) adjacent to the Marquesas fracture zone. Even in the deepest part (> 4300 m) of the basin, sediments still contain from 10 to 30% of $CaCO_3$. Therefore, as previously mentioned, the CCD in the Tiki Basin as well as around the Tuamotu Islands is much deeper than 4300 m and probably close to 4500 m, as indicated by the cores taken in the Tiki Basin (Fig. 2, Appendix Table 1).

The deepest core (KS 09), taken at a depth of 4453 m, consists of pelagic clay containing only traces of calcareous nannoplankton (Appendix Table 2). The shallowest core (KS 08) gives us some indications about the lysocline. The core (Fig. 2, Appendix Table 1) which consists (in its upper part) of calcareous mud relatively rich (< 35%) in well preserved planktonic foraminifera, has been taken close to the lysocline level. Thus the lysocline might be close to 4000 m at that site.

In the Tapu Basin (Figs. 1, 3) no core has been taken. Surface sediments were however obtained during the CNEXO cruise Techno 8 (Appendix Table 1). The sediments sampled were associated with nodule sampling. They were taken at depths from 4690 to 4852 m. Although they are concentrated on the northeastern, they give an idea of the sedimentary facies of the Tapu Basin edge of the basin. The studied sediments are essentially pelagic clay, rich in hydroxides (< 40%) and zeolites (< 15%) and poor in calcareous particles (Appendix Table). Three samples, however, taken around 4750 m water depth contain from 5 to 30% of calcareous nannoplankton. Thus the CCD might be deeper than 4750 m. In fact, during a recent cruise in the easternmost part of the Tapu Basin, we were able to test this hypothesis and to show that the CCD there is very close to 4900 m (SONNE cruise 06.1, unpublished report).

The Aitutaki-Tonga areas (Figs. 4, 5) were surveyed by the ORSTOM Moumea group. The first one is located in the southern part of Penrhyn Basin, between Manihiki Plateau and the Cook Islands. The location of these stations was chosen to complete a preliminary survey carried out in 1976 over the same area by the CCOP/SPOAC[1] Technical Secretariat and the Cook Islands Government.

Other samples were obtained in the southern part of the Samoa Basin, between 20 and 25° S, near the Tonga trench.

The Aitutaki area, located between the Manihiki Plateau, the Society Islands and the Southern Cook Islands (Figs. 2, 5) presents an interesting sediment distribution pattern. Between 4700 and 4800 m water depth, pelagic clays are dominant, but still contain calcareous particles (foraminifera = 1-3%; nannofossils = 1-10%).

At greater depths, the pelagic clays do not contain any more calcareous particles. This shows that the CCD in this area is close to 4800 m or even deeper. Consequently, we propose a CCD level between 4800 and 5000 m.

Considering the pelagic clay composition, we may add that it is enriched in hydroxides (10-25%) and zeolites (5-15%; Appendix Tables 4, 5) around 5000 m water depth (Appendix Table 1). There are two major facies within the Aitutaki area: a pelagic clay rich in zeolites and bearing volcanic glass and siliceous debris, and a pelagic clay relatively rich in siliceous debris and bearing zeolites and volcanic glass. The first one characterizes the area extending north of 13° S. Zeolites are particularly abundant (10-25%) and of relatively large size (< 63 m) and abundance (< 3%). Furthermore,

---

[1] CCOP/SOPAC: Committee for co-ordination of joint prospecting for mineral resources in South Pacific Offshore areas.

this facies is richer than the previous one in radiolarians (5-10%; ex. GT. 204, 211, 213, Appendix Table 4) but much poorer in volcanic glass (< 1%).

Near the Tonga Trench (≈ 23° S; Fig. 5), sediments differ in an obvious way from those of the Aitutaki area by their relative richness in volcanic glass (10-25%) and siliceous debris (< 10%). This increase in siliceous debris probably reflects relative increase in the oceanic fertility.

Evolution of Nodule Distribution and Composition With Respect To Water Depth And Topography

During TRANSPAC cruises (I and II), only few nodules (≈ 3 kg/m^2) were recovered from the Marquesas and Tuamotu areas (Pautot and Hoffert, 1974). However, in the light of our first observations (Pautot and Hoffert, 1974; Pautot and Melguen, 1975, 1976) we suggested that the presence of nodules seemed to be related to the following conditions:

- an old oceanic crust (up to 15 my),
- a moderate thickness of sedimentary cover (less than 100 m),
- a water depth close to the CCD,
- a smooth bathymetry.

In order to substantiate these tentative observations, as well as to define more closely the general relationship between the density and grade of nodules and their oceanic environment, we have studied much new data in each of the areas mentioned. Several hundreds of samples have been taken by the CNEXO/SLN Group and AFERNOD around the Tuamotu Archipelago, the Marquesas Archipelago, along the Marquesas fracture zone, in the Tapu and the Tiki Basins. Location of these samples, density and composition of nodules are not presented here because they are still under industrial secret. We show the evolution of nodule density (concentration on the sea floor) and grade (metal content) with increasing water depth. Nodule abundance was determined using both the weight of the nodules recovered by free-fall grabs and the abundance observed on bottom photographs.

Tuamotu-Marquesas Area (Fig. 1)

The general distribution of nodule abundance with respect to water depth (Fig. 9) in the whole Tuamotu-Marquesas area shows obvious trends.

First of all, no nodules have been found between 0 and 3900 m. Secondly, a decrease of abundance seems to appear at water depths greater than 5000 m. One may note, however, that only very few samples have been taken at such water depth in this area.

High nodule abundance occurs between 4000 m and 5000 m water depth (Fig. 9) with maximum abundance (up to 10 kg/m^2) between 4350 and 4900 m water depth. As the samples are coming from an extensive

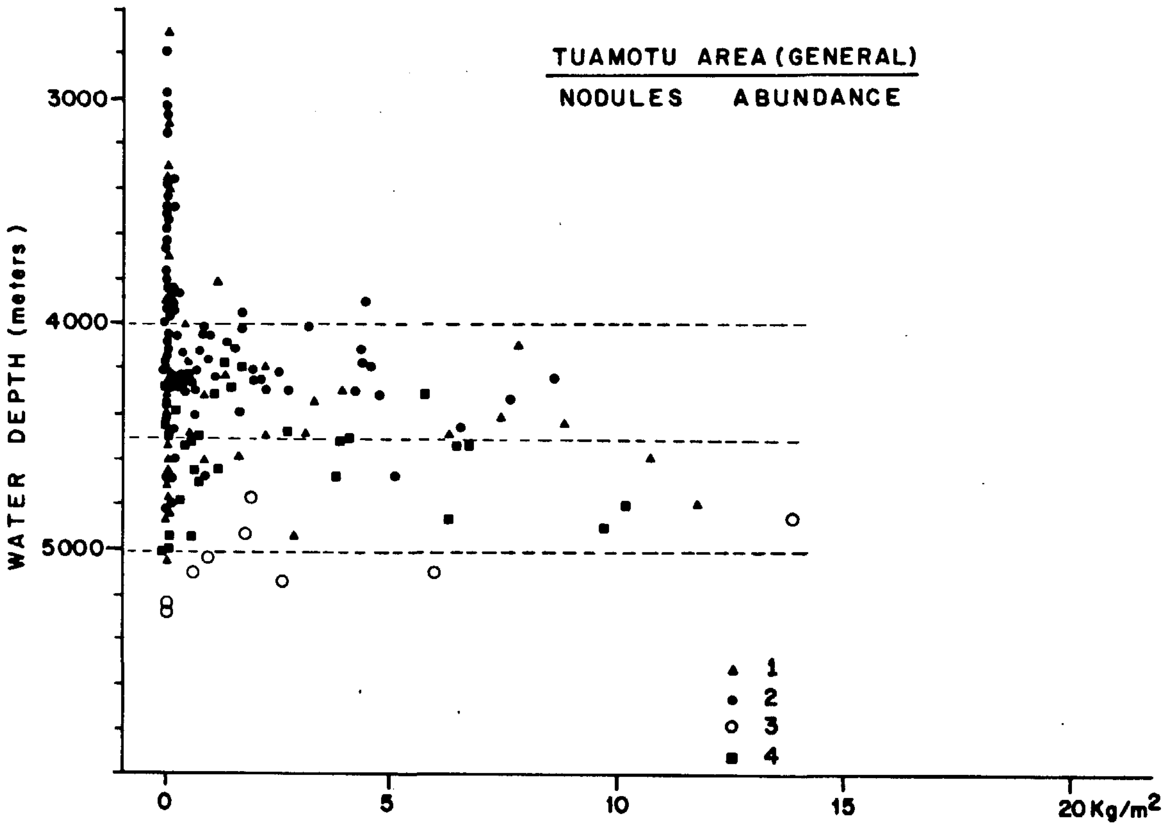

Fig. 9. Nodule abundance versus water depth in the whole Tuamotu-Marquesas area. 1, 2, 3, 4 represent values from four different CNEXO cruises.

area, it is difficult to determine in more detail distribution patterns.

Tiki-Marquesas Area (Figs. 1, 2)

As in the previous area, high nodule abundance is found between 4000 and 5000 m water depth (Fig. 10). South of the Marquesas fracture zone, the nodule distribution is, however, different from that encountered north of this zone. In the Tiki Basin, south of the Marquesas fracture zone, the highest nodule abundances have been found between 4000 m and 4350 m water depth (Fig. 1). North of the Marquesas fracture zone, highest densities are found at greater water depth (4500-4900 m). Above and below these water levels, the nodule abundance decreases drastically.

This analysis underlines some interesting observations:

- in a given morphostructural location, a preferential water depth is associated with the maximum abundance of nodules,
- the nodules are distributed through a range of water depth of about 300 or 400 meters,
- maximum values of abundance are situated in the lower part of this range.

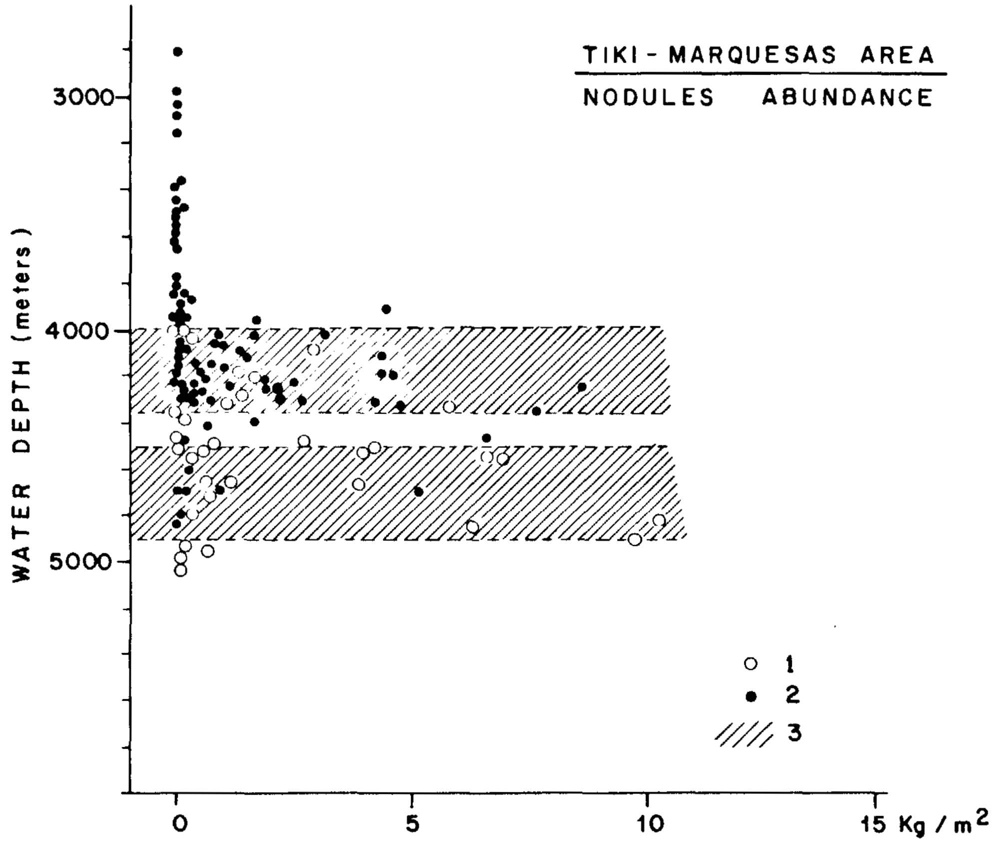

Fig. 10. Nodule abundance versus water depth in the Tiki Basin and North of the Marquesas fracture zone. 1: north of the Marquesas fracture zone; 2: south of the Marquesas fracture zone; 3: zones of highest density south and north of the fracture zone.

Ni and Cu grade do not show the same type of correlation with water depth (Fig. 11 and 12). In the depth interval (4000-4350 m) where nodules are the most abundant, Ni and Cu grade is very scattered. High Ni grade (i.e. about 1.5%) is found between 4100 and 4400 m water depth. There may be an ill-defined trend with a maximum around 4350 m. In this case, maximum abundance values and maximum Ni content are in concordance near 4350 m.

Concerning the distribution of Cu content at increasing water depth, we may also note that the highest values (about 1%) are also scattered between 4000 and 4350 m (Fig. 12), but with a swarm of values around 4300 m.

In brief, the preferential depth for nodule exploration in the Tiki Basin seems to be 4350 m. At this depth, the highest values of nodule abundance and grade converge.

Aitutaki Area (Figs. 4, 5)

Nodule abundance presents a clear maximum between 4800 and 5200 m water depth (Fig. 13) where nodule concentration varies from 5 to

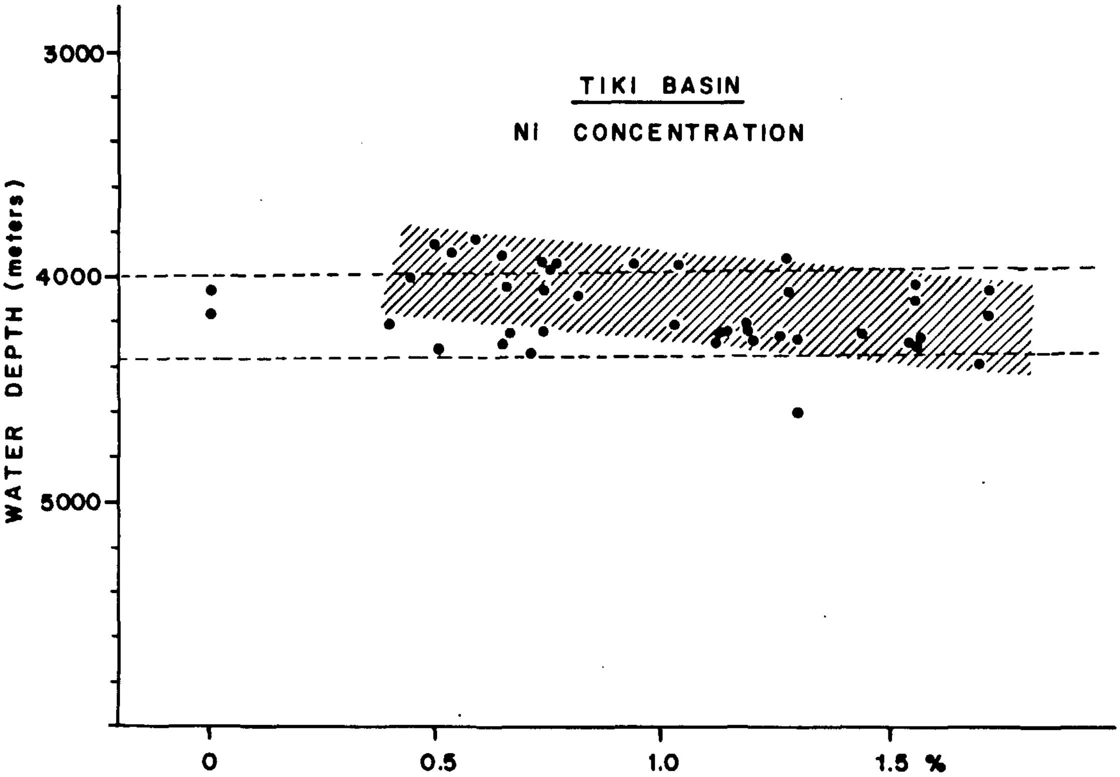

Fig. 11. Nodule composition (= Ni concentration) versus water depth in the Tiki Basin. Highest grade is comprised between 4000 and 4350 m.

25 kg/m^2. Below 5200 m, this concentration decreases markedly. Consequently, the 4800-5200 m depth range appears as being the preferential depth for nodule distribution in the Aitutaki area.

We may note (Fig. 14) that Ni content increases (0.2-1.1%) with increasing water depth, and that Cu values exhibit the same tendency to enrichment with increasing water depth but present lower grade (0.2-0.7%, Fig. 15). Co grade shows no correlation with water depth and presents its highest value at 4800 m and at 5200 m water depth (Fig. 16).

In brief, no concordance appears between maximum nodule abundance and maximum grade in the Aitutaki area.

Tapu Basin (Figs. 1, 3)

The Tapu Basin was studied first on a regional scale and then on a more detailed one.

The regional study being focused on a small area characterized by a relatively constant water depth, we were not able to show a general pattern concerning the nodule distribution in the Tapu Basin. However, it appears that nodule concentrations show great variations (0-10 kg/m^2) and are very scattered within a water depth interval of 200 m (4800-5000 m; Fig. 17). In this interval the Ni + Cu concen-

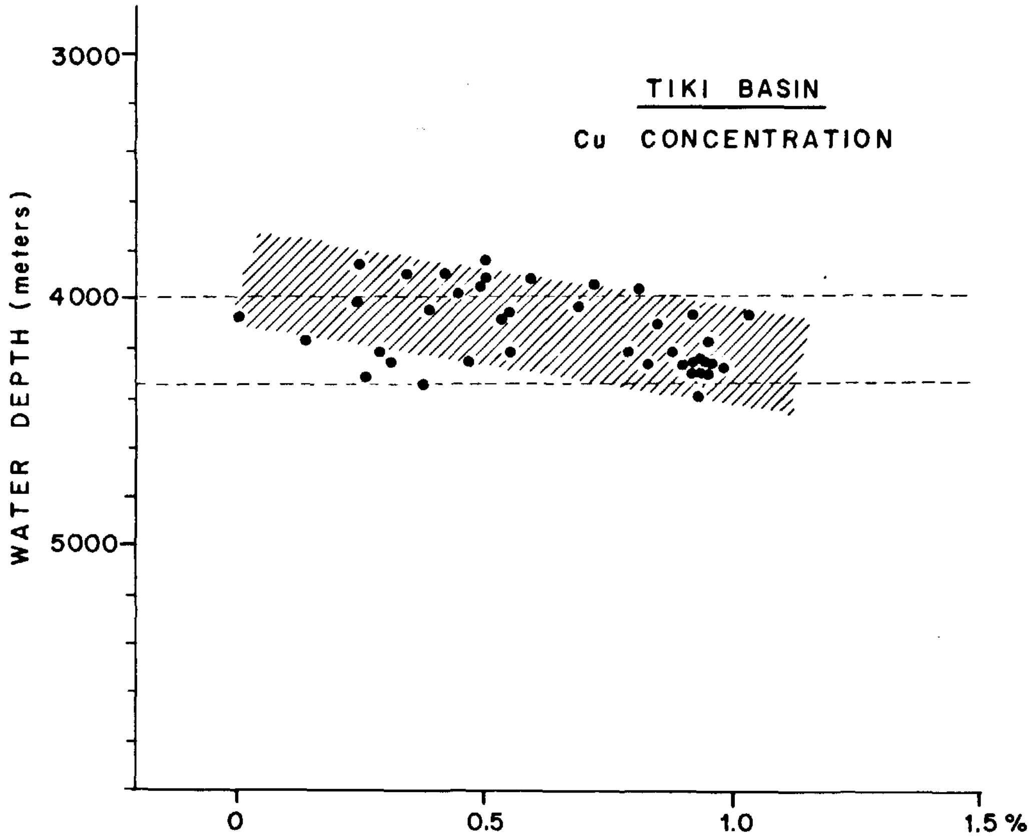

Fig. 12. Nodule composition (= Cu concentration) versus water depth in the Tiki Basin. Highest grade is comprised between 4000 and 4350 m.

tration (Fig. 18) exhibits values around 2% with maximum of 2.5%.

The detailed study was carried out around 7° S and 146° W on the flank of the Tapu Basin, along two crossing traverses. One hundred free-fall grabs were made on each traverse (NS and EW) with a mean spacing of 300 to 500 m.

The stations are regularly spaced on each traverse. In order to simplify the representation of the relationship existing between the nodule distribution and the bottom topography, only the depth of the free-fall grab stations were reported (Figs, 19, 20). Station depths were then joined to each other by a straight line. We thus obtained a schematic representation of the topography along both traverses of the "cross".

The purpose of this detailed study was to compare the nodule characteristics with two associated important factors of the oceanic environment: the depth and the topography of the ocean floor.

Depth and topography of the ocean floor. Mean depth is 4900 m with highs shallower than 4700 m and deeps around 5100 m (Figs, 19, 20). Morphology is smoother and rounder on the NS profile than on the EW profile (Figs. 19, 20). One can distinguish sharp reliefs, rounded hills, perched plateaus, rough relief, valleys.

Nodule abundance along both profiles (Figs. 19, 20A). Nodule

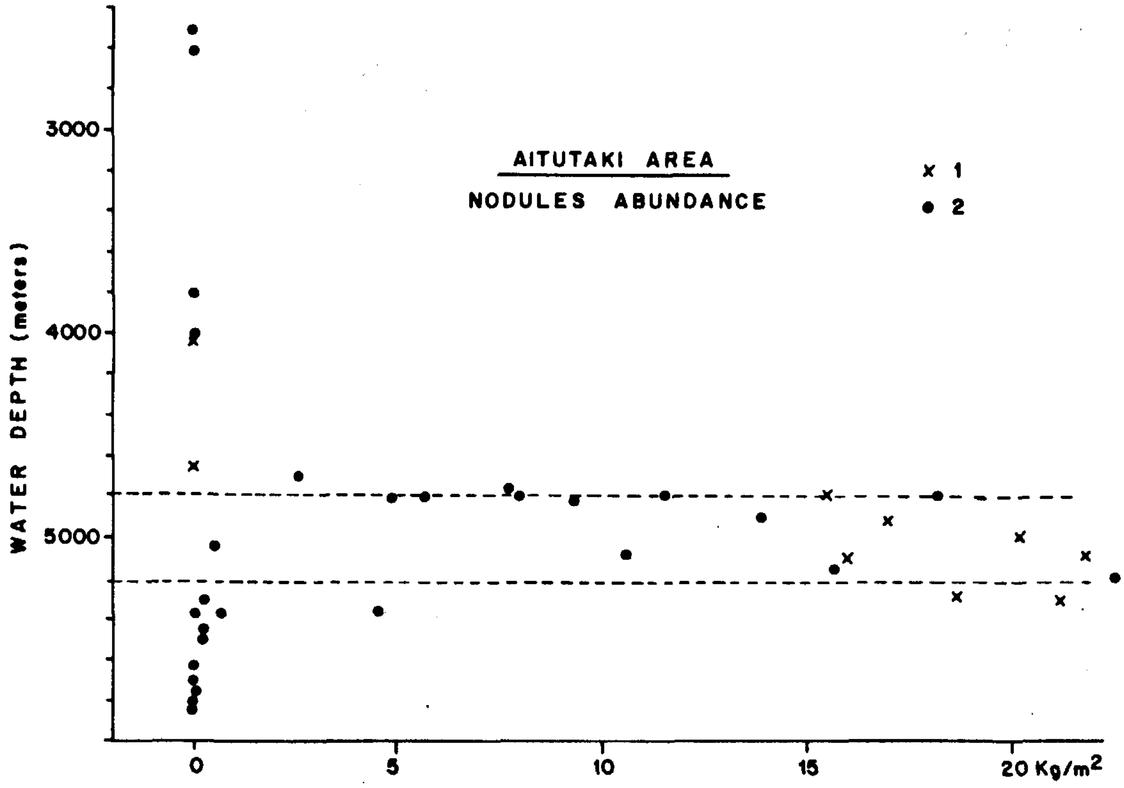

Fig. 13. Nodule abundance versus water depth in the Aitutaki area. 1: data from Landmesser et al. (1976); 2: ORSTOM/CNEXO data. Highest densities between 4800 and 5200 m.

abundance (in areas where they are present) generally varies from 2.5 kg/m^2 to 5.0 kg/m^2 (Figs. 19, 20).

Nodules are rare:

- on steep flanks of hills,
- on low and smooth areas.

Greater abundance is noted:

- on gentle slopes of hills,
- on perched plateaus and in area of rough relief.

The relationship existing between abundance and topography is much clearer along the North-South Profile than along the East-West Profile (Figs. 19, 20).

Nodule grade along both profiles (Figs, 19, 20G). Mean concentrations of Ni + Cu in this area varies from 1.8% to 2.0%. Values are scattered along both profiles, without showing a clear correlation with the topography (Figs. 19, 20). On rough topographic features, however, the nodule grade is lower than along gentle slopes. A profile of stations elsewhere in Tapu Basin (same area) was analyzed by V. Rendard (person. commun.) in order to evaluate the relationship between the bottom morphology and the grade of transition elements (Fig. 21). This approach, element by element, is more refined than the previous one, in which Ni and Cu content was taken as a whole. Figure 21 clearly shows a positive correlation between

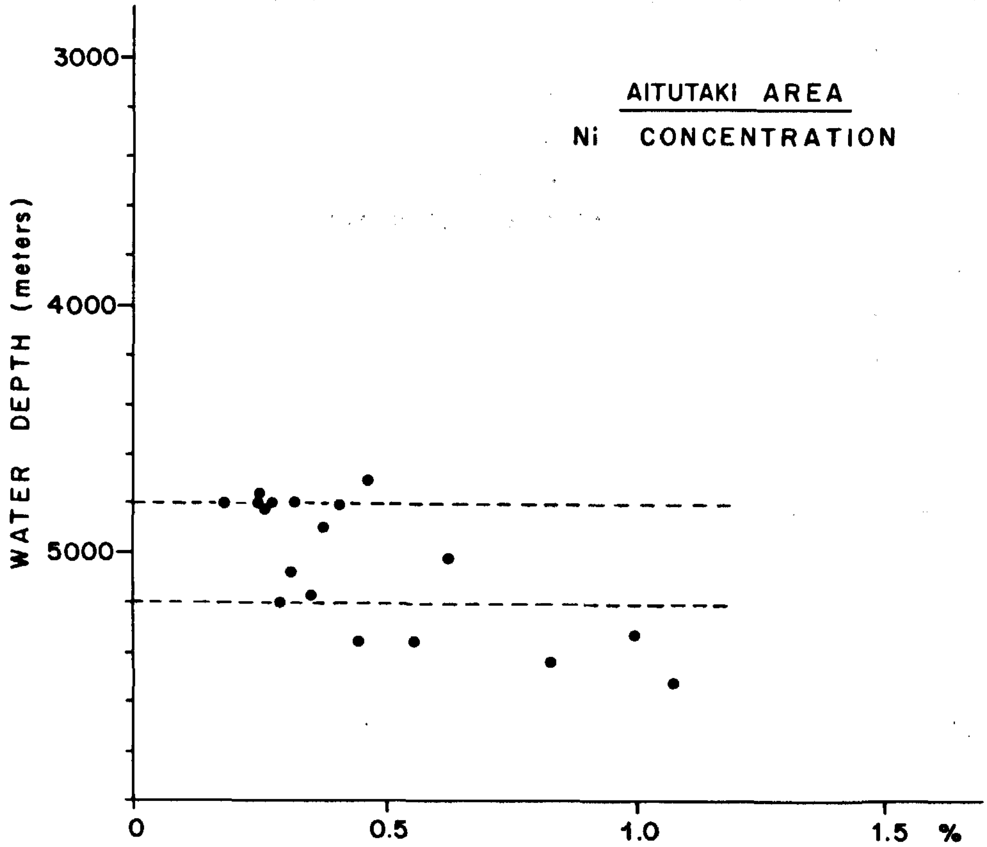

Fig. 14. Nodule composition (= Ni concentration) versus water depth in the Aitutaki area. Highest grade near 5400 m.

Cu grade and topographic lows. The Ni grade is less well correlated with depressed features. Co grade appears opposed to the Cu grade, with higher values on topographic highs. Mn grade appears to follow the same variations as Cu and Ni grade. The enrichment in Cu in topographic lows might be related either to the general enrichment of the nodules in Mn oxides, or to the presence of todorokite which incorporates selectively Ni, Cu and Mn in deep water areas (Cronan and Tooms, 1969; Cronan, 1977).

Nodule size distribution along both profiles (Figs. 19, 20S). By measuring the length of the major axis of the nodules, five classes were determined: class 1 (0 to 1 cm), class 2 (1 to 2 cm), class 3 (2 to 3 cm), class 4 (3 to 4 cm), class 5 (4 to 5 cm).

Classes 1 and 2 are dominant and often associated (Figs, 19, 20). Homogeneous populations (1 and 2) are visible on smooth reliefs or high plateaus with one class dominant (1 or 2), and presence of other nodule types in various proportions. Largest nodules are generally found in depressed areas and valleys. Along sharp reliefs, small nodules (class 1 and 2) are dominant.

Nodule morphology along both profiles (Figs. 19, 20M). The following classification is used in this paper: mononodules, polynodules and debris. Mononodules are coupled or coalescent nodules. Debris which are mainly broken, flattened ovoïd mononodules are

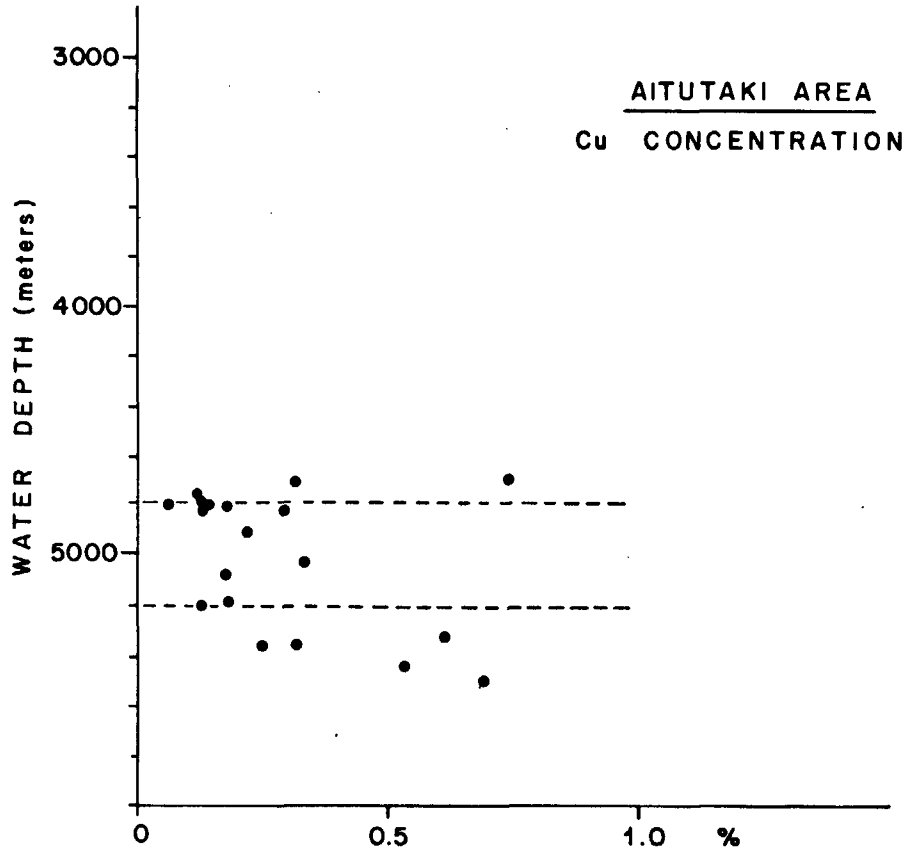

Fig. 15. Nodule composition (= Cu concentration) versus water depth in the Aitutaki area. Highest grade near 6400 m.

largely dominant in this area.

Unbroken ovoïds are present on gentle hills, and irregular nodules are preferentially found on and around topographic highs. Polynodules are seldom observed.

Nodule setting and environment (from bottom photographs). Study of bottom photographs shows that nodules are generally partially buried within the sediments. All photographs emphasize this phenomenon. Furthermore, in certain cases, one can guess the presence of nodules on the bottom only through a small mound sticking out through sediment. Some pictures even give the impression of a fossil nodule field in the process of being buried.

Discussion

In the light of the previous observations, we are now able to draw some general conclusions about the nodule abundance and grade distribution in the Central South Pacific.

First of all, nodules are generally found between 4000 m and 5200 m, and not deeper. They seem to be concentrated in a 300/400 m-thick depth interval. This interval is not everywhere the same but varies from one area to the other, as follows:

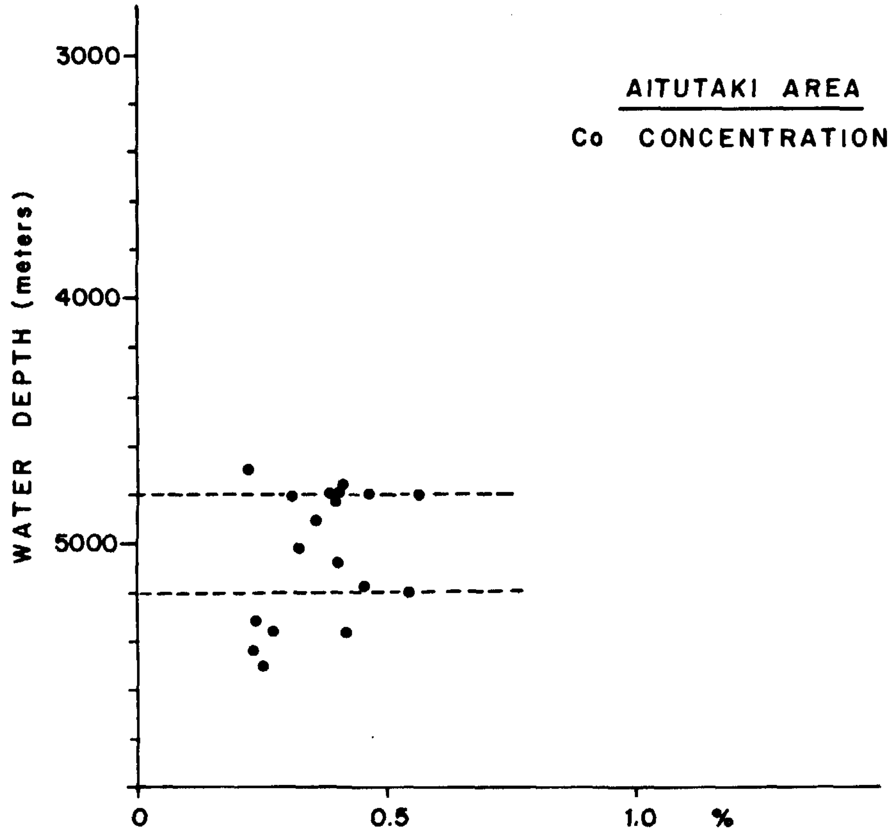

Fig. 16. Nodule composition (= Ni concentration) versus water depth in the Aitutaki area. Highest grade near 5400 m.

4000-4350 m in the Tiki Basin
4500-4800 m north of the Marquesas fracture zone,
4800-5000 m in the Tapu area,
4800-5200 m n the Aitutaki area.

Within this depth range of perferential maximum distribution exists a certain level at which abundance and grade are in good concordance. The abundance parameter is represented by a curve showing a peak in a given 300/400 m-thick interval, with maximum values at base of the peak. The grade parameter is generally represented by a straight line which exhibits a grade increasing with depth.

These two parameters may or may not be in good concordance. The abundance peak may correspond to maximum grade (like Tiki Basin around 4350 m); or the abundance peak may be situated above the maximum grade (like Aitutaki Passage around 5200 m). This conclusion contradicts the observations of Menard and Frazer (1978) for the whole Pacific Ocean.

Water depth plays obviously a major role in the distribution of manganese nodules. Topography of the sea floor appears to be, however, an important secondary factor controlling the abundance as well as the grade of nodules (Figs, 19, 20, 21).

Areas of smooth relief and gentle slopes have the highest density of nodules. Areas of sharp relief are on the contrary, unfavor-

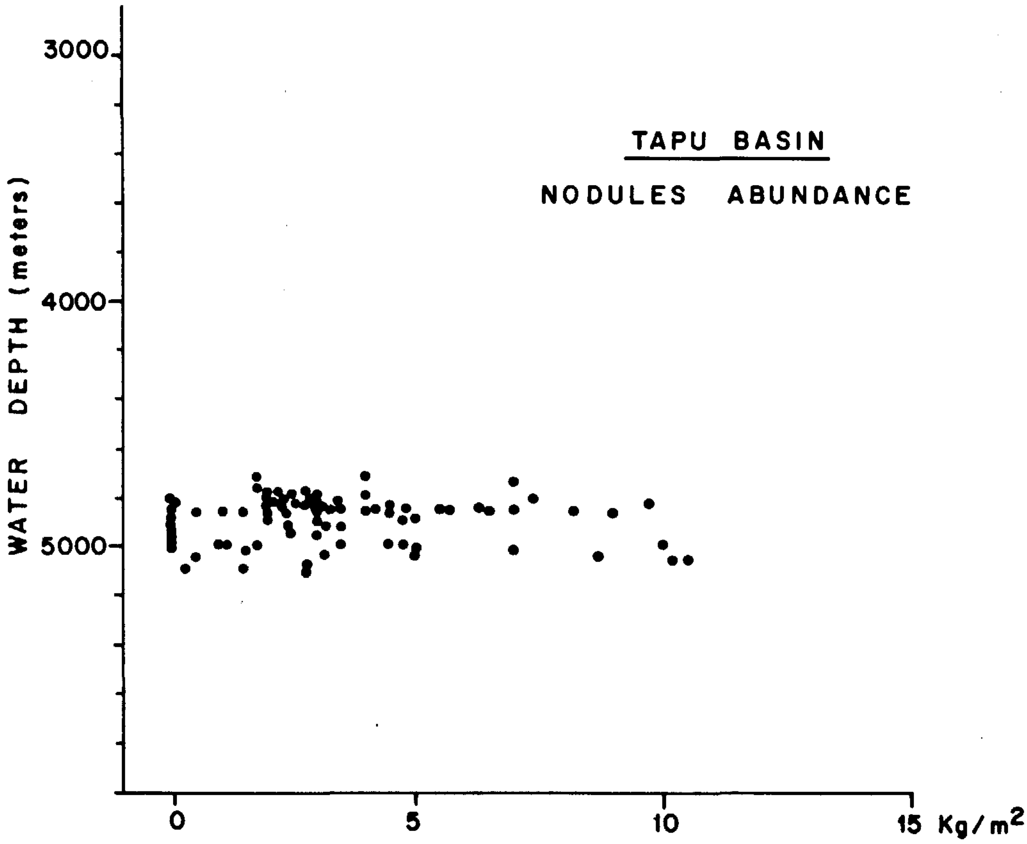

Fig. 17. Nodule abundance versus water depths in the Tapu Basin. Highest density between 4800 and 5000 m.

able in terms of abundance as well as grade. Depressed areas and valleys also have low abundances but present the highest content in Cu.

Therefore, within a 200 m thick depth interval, there are secondary fluctuations which are related to the local topography and are superimposed on major ones that are linked to more regional factors controlling the sedimentary facies, such as the bottom circulation and oceanic fertility.

We have been particularly impressed by the fact that, in most of the cases, the preferential depth of nodule distribution was not only below the Benthic Front and therefore within the Pacific Bottom Water mass (Fig. 7), but generally within the depth interval separating the calcite lysocline from the Calcite Compensation Depth (CCD). The concept of the lysocline, implicit in the findings of Peterson (1966), Berger (1967), Ruddiman and Heezen (1967), was introduced to denote a surprisingly well defined facies boundary zone between well preserved and poorly preserved foraminiferal assemblages on the floor of the Atlantic Ocean (Berger, 1968), and on that of the South Pacific (Berger, 1970a, Parker and Berger, 1971). The lysocline is generally envisaged as the level at which there is a maximum change in the composition of calcareous fossil assemblages due to differential dissolution. In areas of low oceanic fertility, such

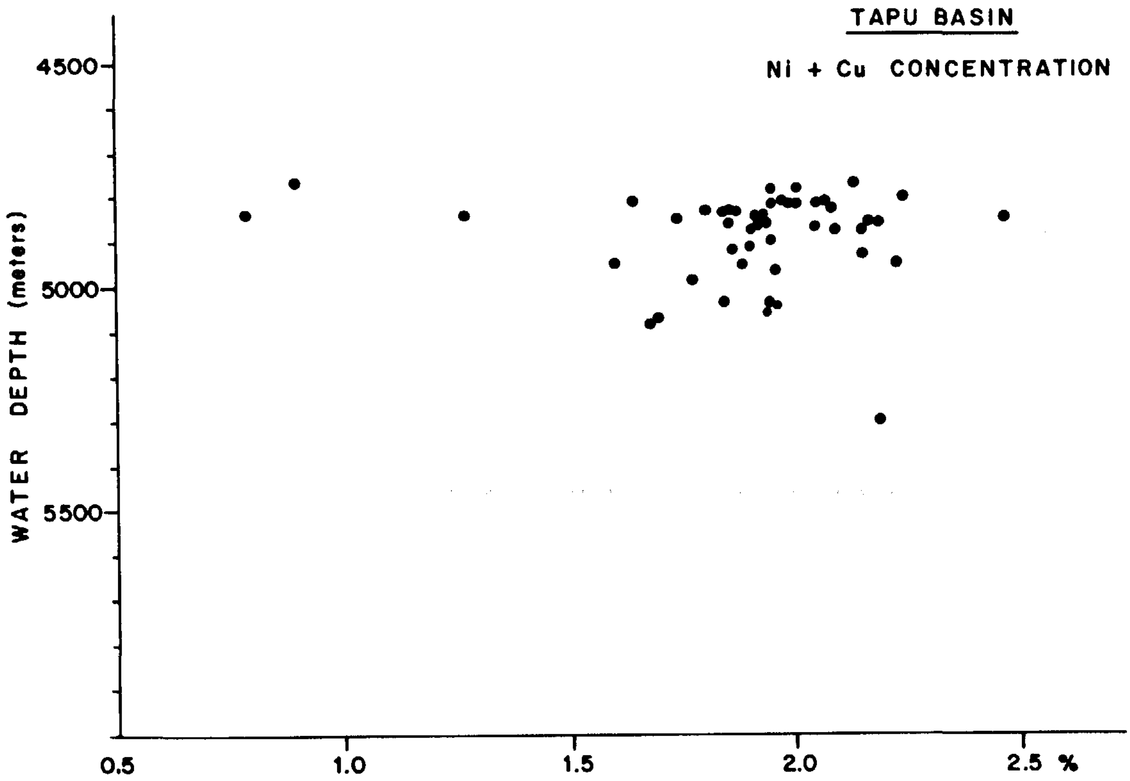

Fig. 18. Nodule composition (= Ni + Cu concentration) versus water depth in the Tapu Basin. Highest concentrations are scattered between 4700 and 5200 m.

as related to the aggressiveness of the bottom water masses, the lysocline corresponds to the "hydrographic lysocline" as defined by Peterson (1966).

In the Central South Pacific the lysocline is close to 4000 m (Berger, 1970b, 1971, 1976; Parker and Berger, 1971; Roth and Berger, 1975, Berger et al., 1976), and therefore well beneath the Benthic Front which marks the level at which the dissolution of foraminifera is first obvious (Berger, 1976). The sharpness of the transition zone from high to low values of carbonate varies from area to area, with a mean value of 300 m in the studied area (Berger et al., 1976). According to Berger et al. (1976), the CCD in the Tiki, Tapu and Aitutaki areas, varies between 4200 m and 5000 m (Fig. 22, a and b). Berger's values are not in complete agreement with our observations, according to which we propose the following CCD values:

4500 m for the Tiki Basin
4900 m for the Tapu Basin
4800-5000 m for the Atiutaki-Tonga area.

The discrepancy between the estimates of Berger et al. (1976) and ours could be explained partly by the fact that Berger et al. considered the 10% $CaCO_3$ level as being the CCD level, and partly because the density of our data in the given areas is locally greater than Berger's.

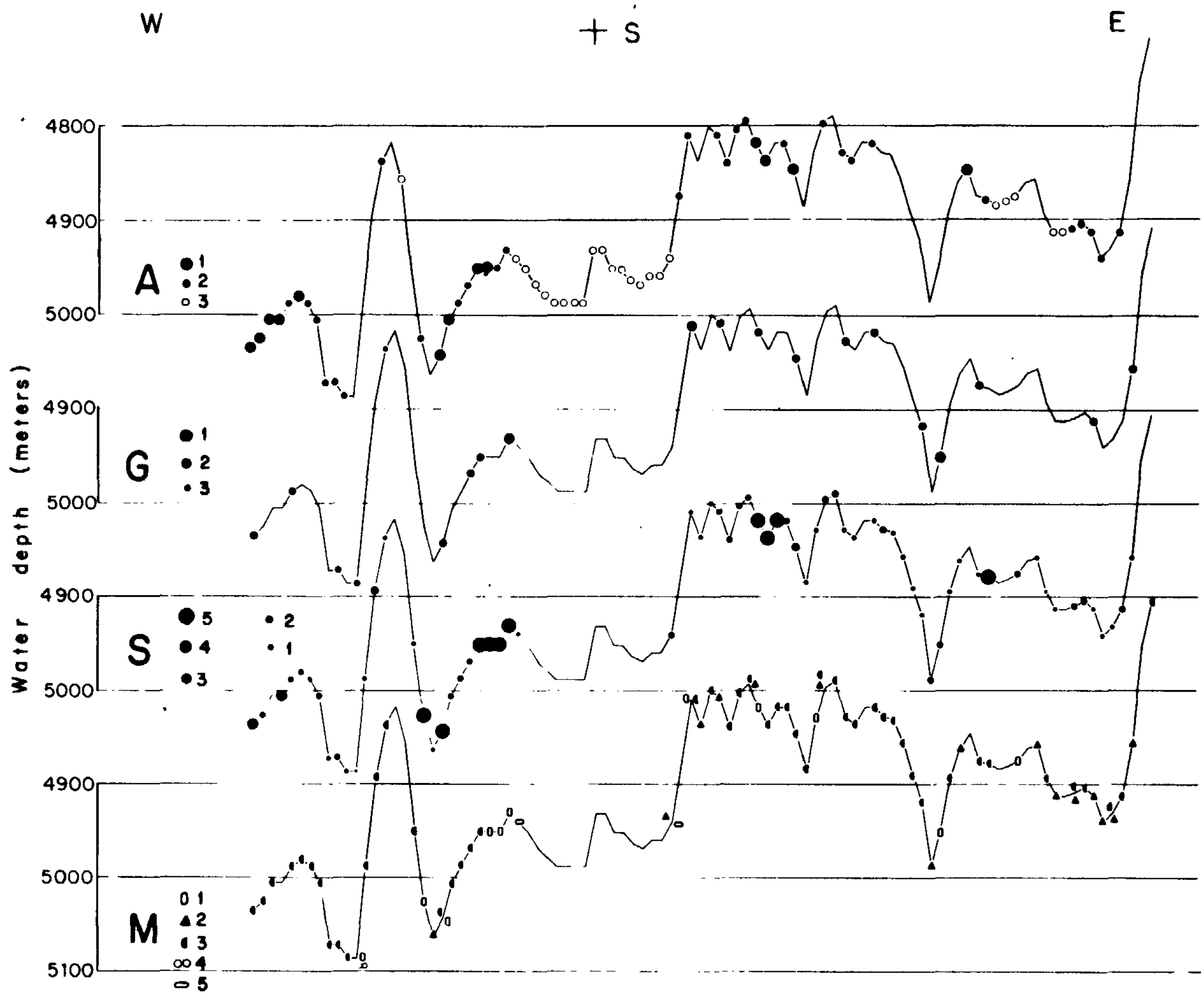

Fig. 19. Detailed study along a west-east profile in the Tapu Basin. Relationship between water depth, topography and: nodule abundance, grade, size, morphology.

A (abundance): 1. density ≥ 5 kg/m^2; 2. density comprised between 2.5 and 5 kg/m^2; 3. no nodules.

G (Ni + Cu grade): 1. grade ≥ 2.0%; 2. grade comprised between 2.0 and 1.8%; 3. grade comprised between 1.8 and 1.5%.

S (size): 1 to 5. nodules size increasing from class 1 (0-1 cm) to class 5 (4-5 cm).

M (morphology): 1. nodules of ovoïd shape; 2. nodules of irregular shape; 3. nodules debris; 4. coupled nodules or polynodules; 5. nodules of geoïd shape.

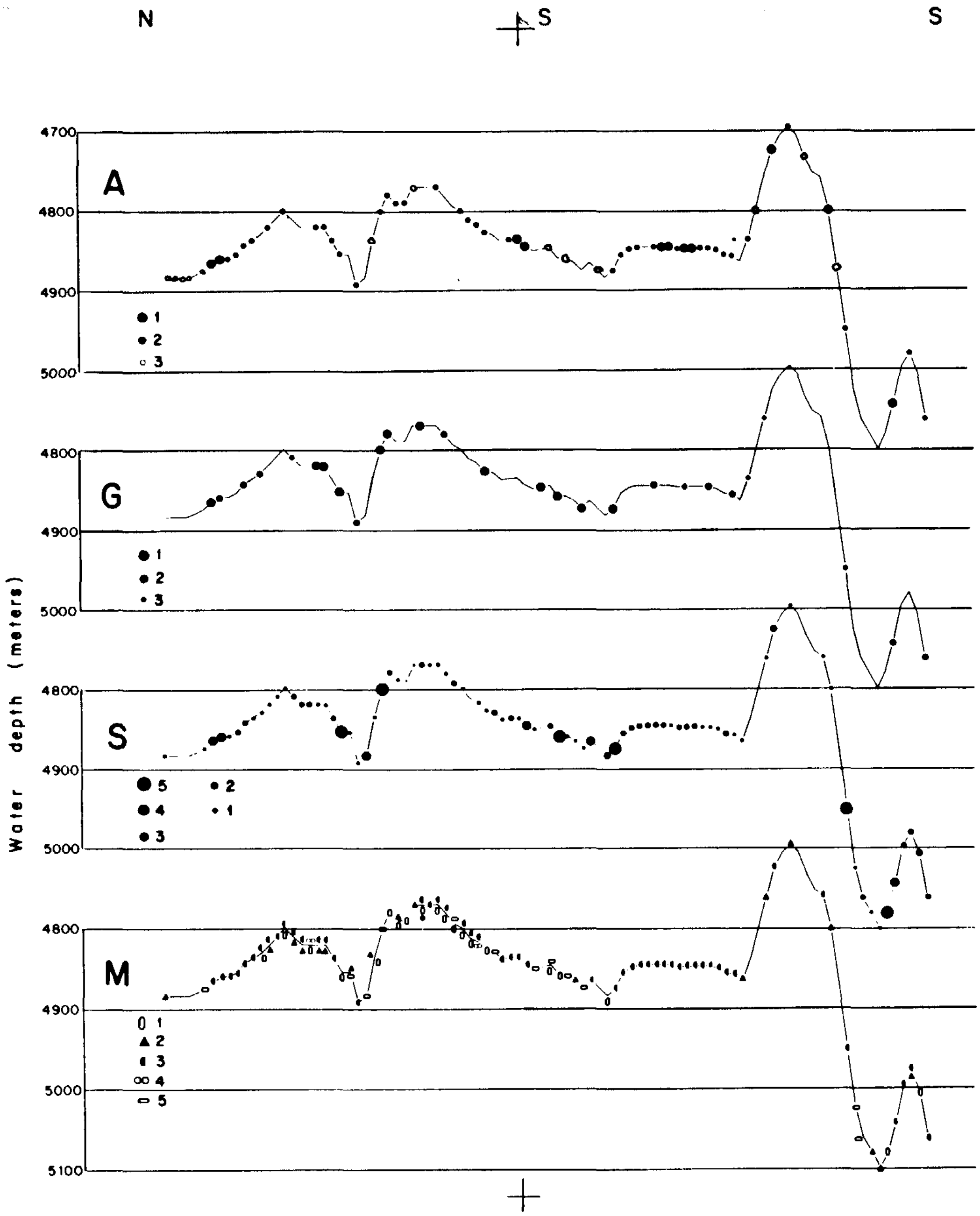

Fig. 20. Detailed study along a north-south profile in the Tapu Basin. Relationship between water depth, topography and: nodule abundance, grade, size, morphology.

A (abundance): 1. density $\geq$ 5 kg/m^2; 2. density comprised between 2.5 and 5 kg/m^2; 3. no nodules.

G (Ni + Cu grade): 1. grade $\geq$ 2.0%; 2. grade comprised between 2.0 and 1.2%; 3. grade comprised between 1.8 and 1.5%.

S (size): 1 to 5. nodules size increasing from class 1 (0-1 cm) to class 5 (4-5 cm).

M (morphology): 1. nodules of ovoïd shape; 2. nodules of irregular shape; 3. nodule debris; 4. coupled nodules or polynodules; 5. nodules of geoïd shape.

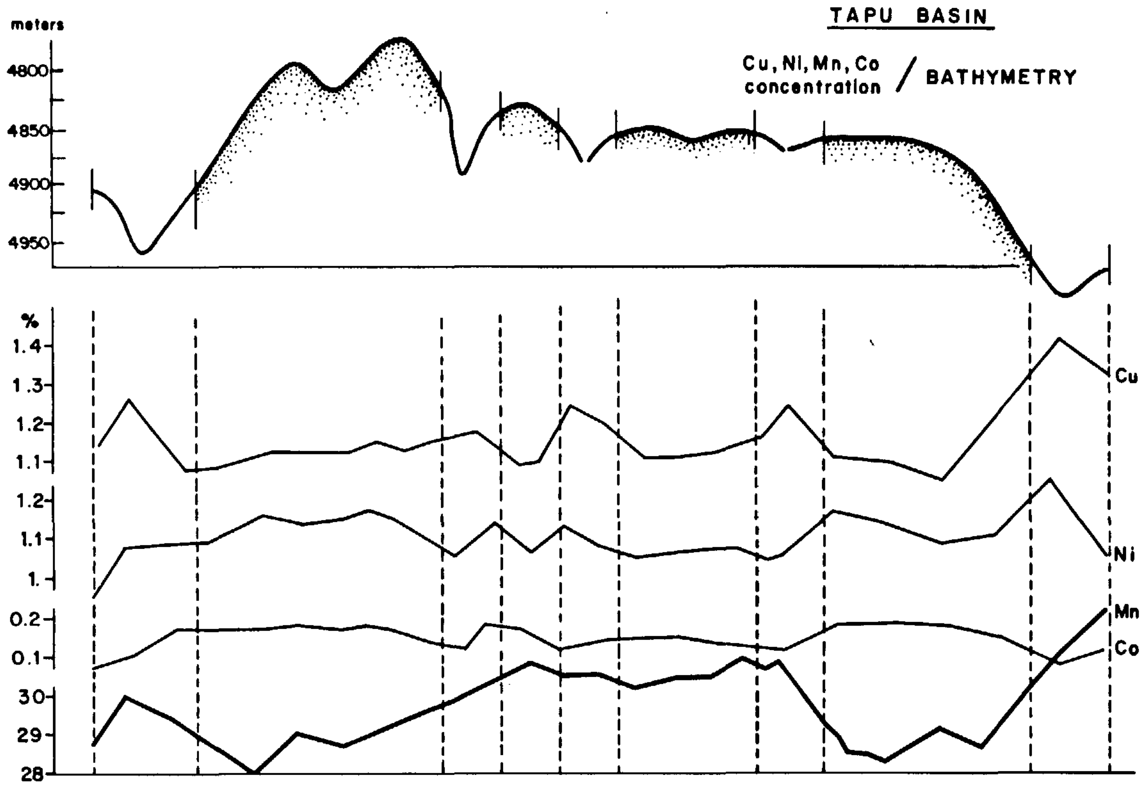

Fig. 21. Detailed study by V. Renard (pers. commun.) of the relationship between topography and nodule grade (Cu, Ni, Mn, Co content) within the Tapu Basin.

Conclusion

Our hypothesis concerning the nodule distribution is based mainly on our CCD estimates. We conclude that in the Central South Pacific, manganese nodules are found within a preferential depth interval, between the hydrographic lysocline and the calcite compensation depth, and that they are concentrated within a very specific sedimentary facies, called the "N-facies" (Fig. 22c).

This so-called "N-facies" or "nodule-rich facies" corresponds to the "R-facies" defined by Berger (1976) as being a residual facies greatly enriched in dissolution-resistant foraminifera species. Bottom Water Circulation and carbonate dissolution seem to be the major controlling factors of this distribution, while bottom topography appears to play a secondary role.

This conclusion dealing with the Marquesas-Tonga area in the South Pacific might not be applicable, for example, to the Clarion-Clipperton area in the North Pacific.

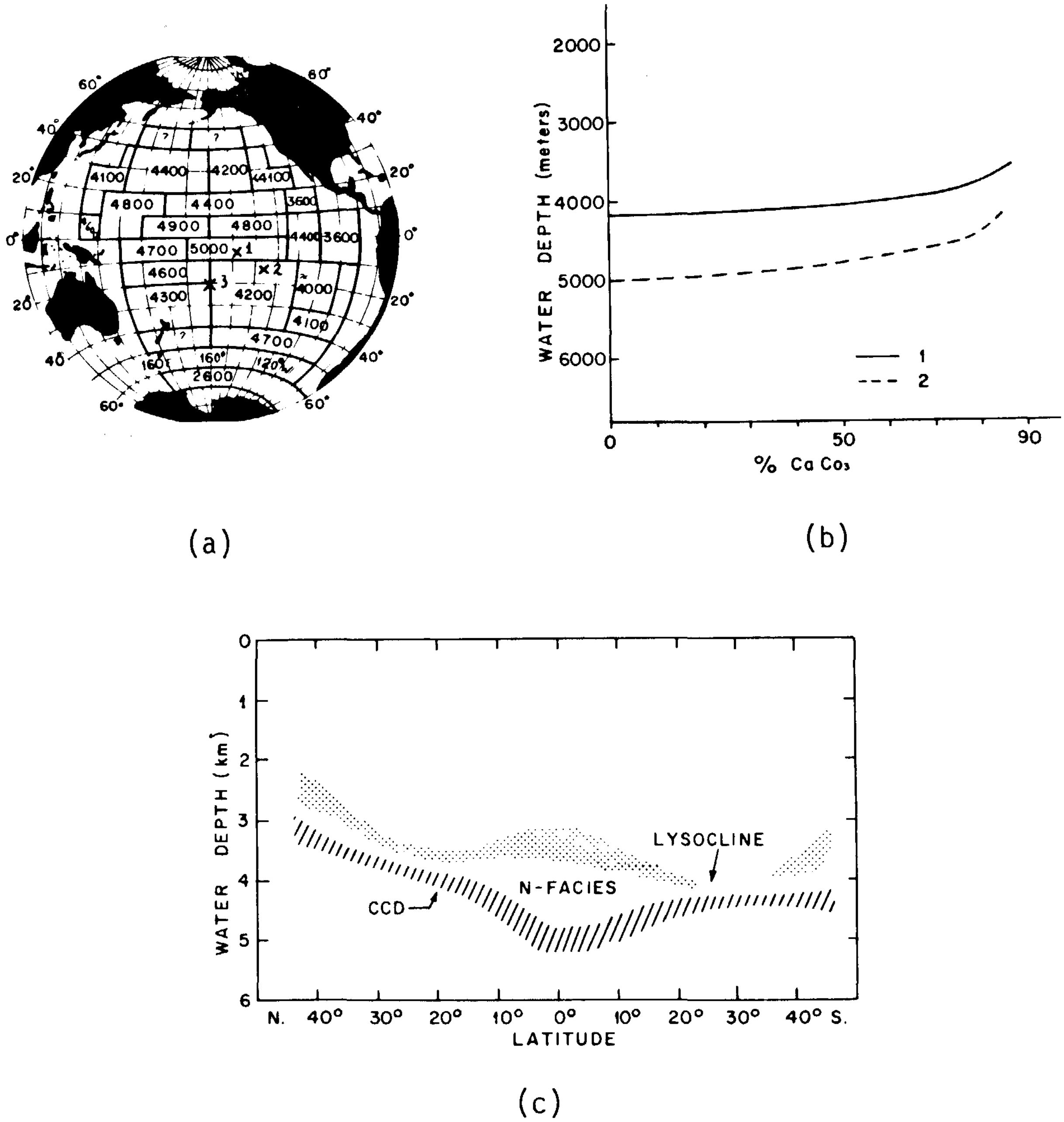

Fig. 22. a) fluctuations of the CCD levels (in meters) in the whole Pacific Ocean. 1. Tapu Basin; 2. Tiki Basin; 3. Aitutaki-Tonga area. After Berger et al. (1976).
b) distribution of $CaCO_3$ content in the sediment at increasing water depth, after Berger et al (1976); 1. Tiki Basin area 2 on Fig. 22a; 2. Tapu Basin, area 1 on Fig 22a.
c) Model of foram dissolution facies (lysocline and CCD) in a N-S profile through the central Pacific (after Berger, 1976). The "N-facies" or "nodules-rich facies" corresponds to the "R-facies" (residual facies greatly enriched in resistant foraminifera species) of Berger (1976, p. 313).

Acknowledgements

We are particularly grateful to AFERNOD and to our colleagues of CNEXO Applied Geology team for allowing us to use nodule data they gathered in the South Pacific. We also thank our colleagues of the ORSTOM Noumea team, who kindly sent sediment samples and analysis of nodules taken in the Aitutaki-Tonga area, during their cruises GEOTRANSIT II and EVA III.

We express our thanks to Dr. V. Renard for the detailed study done in the Tapu Basin during the CNEXO cruise TECHNO 08. We also thank A. Vangriesheim for the compilation done on bottom circulation in the South Pacific, R. Kerbrat, S. Marques for technical assistance, R. Thirion and A. Grotte for drawing the figures. Finally we are particularly grateful to Y. Potard and N. Guillo for so carefully typing the manuscript.

References

Berger, W. H., (1967) Foraminiferal ooze: solution at depths, Science 156, 383-385.

Berger, W. H., (1968) Planktonic foraminifera: selective solution and paleoclimatic interpretation, Deep-Sea Res. 15, 1, 31-43.

Berger, W. H., (1970a) Biogenous deep-sea sediments: fractionation by deep-sea circulation, Geol. Soc. Amer. Bull. 81, 1385-1402.

Berger, W. H., (1970b) Planktonic foraminifera, selective solution and the lysocline, Marine Geology 8, 38-111.

Berger, W. H., (1971) Sedimentation and planktonic foraminifera, Marine Geology 11, 325-358.

Berger, W. H., (1974) Deep-sea sedimentation, In Burk, C. A., and Drake, C. L., eds., The Geology of Continental Margins, Springer, New York, 213-241.

Berger, W. H., (1976) Biogenous deep-sea sediments: production, preservation and interpretation, In Riley, J. R., and Chester, R., eds., Chemical Oceanography 2nd Ed. Academic Press, London, 5, 29, 265-387.

Berger, W. H., Adelseck, C. G., Mayer, L. A., (1976) Distribution of carbonate in surface sediments of the Pacific Ocean, J. of Geophysical Res. 81, 15, 2617-2627.

Bolli, H. M., Ryan, W. F. F., et al., (1978) Initial Reports of the Deep Sea Drilling Project, Washington, D.C., U.S. Government Printing Office.

Craig, H., Chung, Y., and Fiadeiro, M., (1972) A benthic front in the South Pacific, Earth and Planetary Sci. Letters, 16, 50-65.

Cronan, D. D., (1977) Deep-sea nodules: distribution and geochemistry, In Glasby, G. P., ed., Marine Management Deposits, Elsevier, Amsterdam, 11-44.

Cronan, D. S., and Tooms, J. D., (1969) The geochemistry of manganese nodules and associated pelagic deposits from the Pacific and Indian Oceans, Deep-Sea Res. 16, 335-359.

Duncan, R. A., McDougall, I., (1974), Migration of volcanism with time in the Marquesas Islands, French Polynésie, Earth and Planetary Sci. Letters 21, 414-420.
Edmond, J. M., (1971) An interpretation of the calcite spheres experiment (abs.), EOS (Trans. Am. Geophys. Union) 52, 256 p.
Edmond, J. M., Chun , Y., and Sclater, J. G., (1971) Pacific bottom water: penetration east around Hawaii, Journ. of Geophys. Res. 76, 8089-8097.
Heath, G. R., and C. Clu erson, (1970) Calcite: degree of saturation, rate of dissolution and the compensation depth in the deep oceans, Geol. Soc. of Amer. Bull. 81, 3157-3160.
Hoffert, M., Karpoff, A. M., Schaaf, A., and Wirrmann, D., (1978) Caractéristiques sédimentologiques, minéralogiques, biostratigraphiques et géochimiques des sédiments de surface des zones prévues pour les missions Copano. Unpublished Report, Labor. de Géologie de Strasbourg.
Hollister, C. D., Johnson, D. A., Lonsdale, P. F., (1974) Current-controlled abyssal sedimentation: Samoan Passage, Equatorial west Pacific, The Journal of Geology 82, 3, 275-300.
Johnson, D. A., (1972) Ocean-floor erosion in the Equatorial Pacific, Geol. Soc. of Amer. Bull. 83, 3121-3144.
Landmesser, C. W., Kroenke, L. W., Glasby, G. P., Sawtell, G. H., Kingan, S., Utanga, A., Cowan, G., (1976) Manganese nodules from the South Penrhyn Basin, Southwest Pacific South Pacific Marine Geological Notes, Technical Secretariat, CCOP-SOPAC, Suva, 1, 3, 17-40.
Mammerickx, J., Detrick R., and Schlater, J. G., (1972) Fracture zones and magnetic lineations in the South Central Pacific, Publ. by the Institute of Marine Resources, Univ. of California, San Diego, La Jolla BP 529.
Mammerickx, J., Anderson, R. W., Menard, H. W., and Smith, S. M., (1975) Morphology and tectonic evolution of the East Central Pacific, Publ. by the Institute of Marine Resources, Univ. of California, San Diego, La Jolla, BP 529.
Martini, E., (1971) Standard Tertiary and Quaternary calcareous nannoplankton zonation, In Farinacci, A., ed., Roma Proceed. of the II Planktonic Conference Roma 1970, 739-785.
Menard, H. W., (1964) Marine Geology in the Pacific, McGraw Hill, New York, 271 p.
Menard, H. W., and Frazer, J. Z., (1978) Manganese nodules on the sea floor: inverse correlation between grade and abundance, Science 199, 969-970.
Monti, S., and Pautot, G., (1974) Cinq cartes bathymétriques au 1/1 000 000: Tahiti, Raroia, Marquises, Hao, Mururoa. Cartes éditées par le CNEXO, en vente au BRGM.
Parker, F. L., and Berger, W. H., (1971) Faunal and solution patterns of planktonic foraminifera in surface sediments of the South Pacific, Deep-Sea Res. 18, 73-107.
Pautot, G., and Hoffert, M., (1974) Pacifique Sud-Est: cadre structural, morphologique et sédimentaire. Relations avec les nodules

polymétalliques, IIème Colloque International sur l'Exploitation des Océans, Bordeaux, France, 1-4 octobre 1974, 4, BX202, 8 pp., 3 figs.

Pautot, G., and Hoffert, M., (1974) Extension du flanc nord de l' Archipel des Touamotou: analyse structurale et sédimentologique, 2ème Réun. Ann. Sc. de la Terre, Montipellier 310.

Pautot, G., and Melguen, M., Courants profonds, hiatus sédimenentaires et nodules polymétalliques, IXème Congrès International de Sédimentologie, Nice (France), 8, 57-64.

Pautot, G., and Melguen, M., (1976) Deep bottom currents, sedimentary hiatuses and polymetallic nodules, Technical Bull. CCOP-SOPAC n° 2 54-61.

Peterson, M. N. A., (1966) Calcite: rates of dissolution in a vertical profile in the central Pacific, Science 154, 1542-1544.

Reid, J., Stommel, H., Dixon, Stroup, E., Warren, B. A., (1968) Detection of a deep boundary current in the Western South Pacific Nature 217, 937.

Reid, J. L., and Lonsdale, P. F., (1974) On the flow of water through the Samoan Passage, J. of Phys. Oceanog. 4, 58-73.

Roth, P. H., and Berger, W. H., (1975) Distribution and dissolution of coccoliths in the South and Central Pacific, In Sliter, W., Bé, A. W. H., and Berger, W., eds., Dissolution of Deep-Sea Carates, Spec. Publ. Cushman Foundation for Foraminiferal Res. 13, 11-26.

Ruddiman, W. F., and Heezen, B. C., (1967) Differential solution of planktonic foraminifera, Deep-Sea Res. 14, 801-808.

Terry, R. D., and Chillinger, E. V., (1955) Charts for estimating percentage composition of rocks and sediments, J. Sediment. Petrol. 25, 229-234.

Wooster, W. S., and Volkman, G. H., (1960) Indications of Deep Pacific circulation from the properties at five kilometers, J. of Geophys. Res. 65, 4, 1239-1249.

Wong, C. S., (1972) Deep zonal water masses in the Equatorial Pacific Ocean inferred from anomalous oceanographic properties, J. of Geophys. Res. 77, 36, 7196-7202.